Improving the Performance of Classifiers in High-Dimensional Remote Sensing Applications: An Adaptive Resampling Strategy for Error-Prone Exemplars (ARESEPE)

Charles M. Bachmann, *Member, IEEE*

***Abstract*—In the past, "active learning" strategies have been proposed for improving the convergence and accuracy of statistical classifiers. However, many of these approaches have large storage requirements or unnecessarily large computational burdens and, therefore, have been impractical for the large-scale databases typically found in remote sensing, especially hyperspectral applications. In this paper, we develop a practical on-line approach with only modest storage requirements. The new approach improves the convergence rate associated with the optimization of adaptive classifiers, especially in high-dimensional remote sensing data. We demonstrate the new approach using PROBE2 hyperspectral imagery and find convergence time improvements of two orders of magnitude in the optimization of land-cover classifiers.**

***Index Terms*—Active learning, active sampling, barrier islands, hyperspectral, land-cover classification, Virginia Coast Reserve.**

I. Introduction and Background

STOCHASTICALLY optimized classifiers are widespread in remote sensing applications. From researchers who design their own automatic classification algorithms to those who use commercially available packages such as ENVI [5], stochastic optimization is at the core of many of these algorithms, which include, for example, vector quantization algorithms and neural networks. Many of these algorithms have significant optimization times or are prone to problems with local minima. Some of these problems can be overcome by replacing completely stochastic sampling with a more active sampling strategy, or "active learning."

The subject of "active learning" has been studied by a number of researchers [7], [9], [12], [15]. The basic concept is that training in stochastic optimization routines is inherently inefficient, and that selective presentation of patterns within the context of random sampling can lead to faster convergence and, in many instances, better solutions. In [12], it was shown that by choosing samples that lie within a particular distance from current decision boundaries, convergence to the optimal solution is guaranteed, and simple low-dimensional examples were used to prove that their approach could accelerate the rate of convergence for a popular vector quantization known as learning vector quantization (LVQ) [11]. In the later stages of optimization, their approach is intuitively appealing because it suggests that the majority of errors occur near decision boundaries and that that is where the majority of refinements of the decision boundaries should be concentrated. Nevertheless, although this is better than naive stochastic sampling, it may be too restrictive in the early stages of optimization when the decision boundaries are not necessarily in close proximity to their optimal positions. Therefore, there may be a more general approach that leads to faster convergence, a subject which we address in this paper. Before proceeding, we should note that Foody [6] previously discussed how the spatial distribution of patterns chosen for a training set impacts the final generalization of statistical classifiers in remote sensing applications. His recommendation was to design algorithms that would overcome the bias of many classifiers toward patterns in the class cores, by including more border patterns. The approach that we present here does exactly that.

In many of the approaches cited above, illustrative data usually have been low dimensional, and in some cases artificially constructed. A number of the previous approaches to active learning are also slow, especially for high-dimensional applications such as hyperspectral imagery. For example, the multipoint search method described in [7] requires an integral over expressions involving second-order derivatives (Fisher information matrices) and is, therefore, significantly more complicated and computationally expensive than the expressions which govern the approach that we have developed. Likewise, some algorithms have been designed around a specific algorithm such as in [15], in which a complicated scheme of potential pattern interference must also be estimated as the model complexity grows. Similarly, the approach defined in [9] also involves significant computational overhead, primarily from an inversion process which itself is implemented as a stochastic gradient descent algorithm; their approach also uses

Manuscript received October 18, 2002; revised May 29, 2003. This work was supported under the Office of Naval Research under Contracts N0001400WX40016, N0001401WX40009, and N0001402WX30017. Computing resources were provided by the Department of Defense High Performance Computing (HPC) Modernization Program, including the following HPC centers: SMDC, the MHPCC, and the ARL MSRC.

The author is with the Remote Sensing Division, Naval Research Laboratory, Washington, DC 20375 USA (e-mail: bachmann@nrl.navy.mil).

Digital Object Identifier 10.1109/TGRS.2003.817207

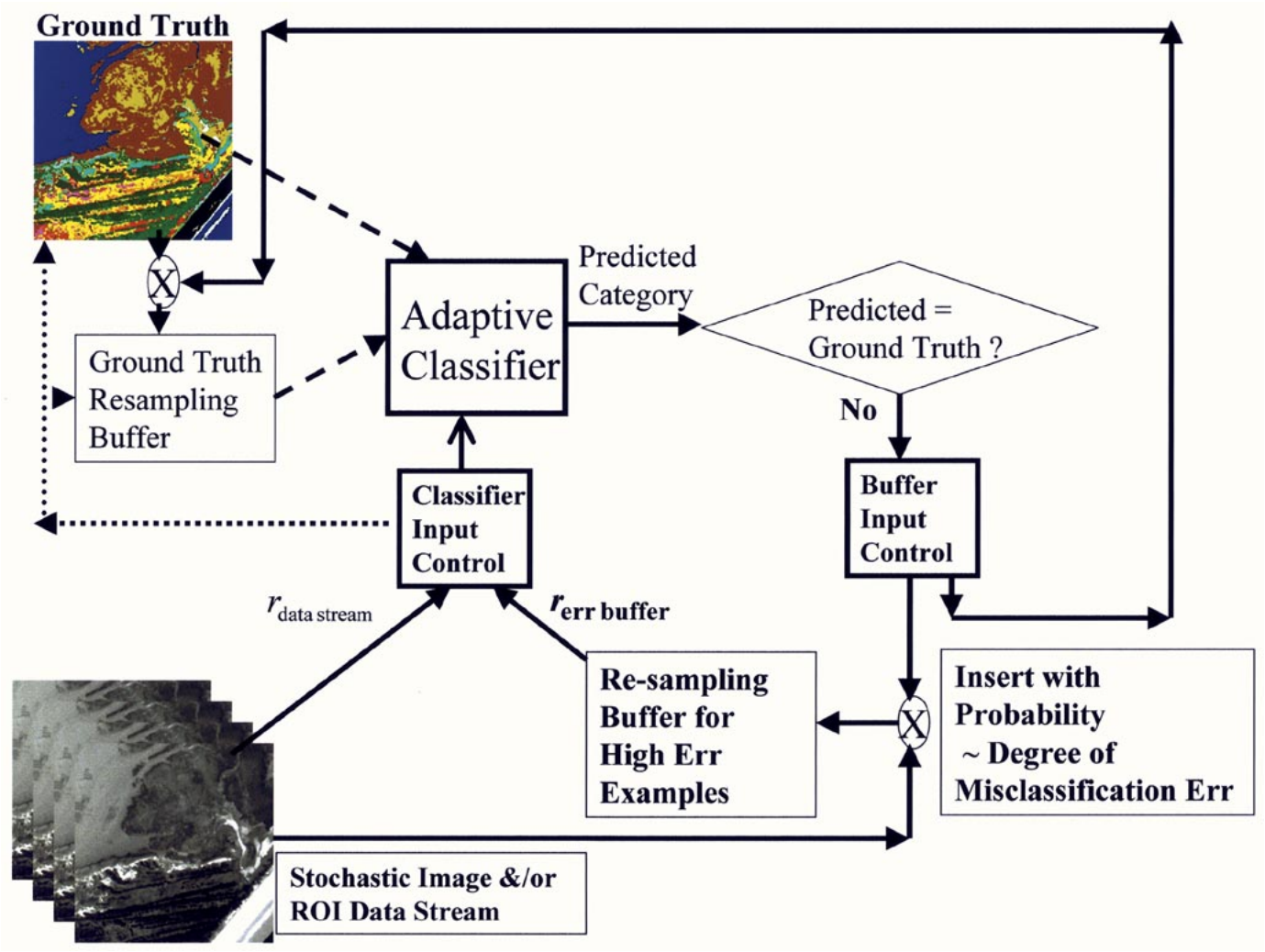

Fig. 1. Schematic diagram of ARESEPE. The input control to the classifier draws samples from the stochastic image stream and the resampling buffer with rates $r_{\text{data stream}}$ and $r_{\text{data buffer}}$. Patterns producing error enter the resampling buffer with probability proportional to degree of asymptotic multiclass misclassification error.

conjugate pairs of pseudopatterns that also must be estimated. This inversion process, thus, requires significant computational overhead, and their entire approach is specific to a particular neural network algorithm. In contrast, the approach defined below is applicable to the optimization of a broad range of statistical classifiers and is implementable online, with minimal computational overhead and storage requirements.

II. Adaptive Resampling Strategy for Error-Prone Exemplars (ARESEPE)

A. Schematic Overview

Our requirement for when data should be resampled is more general than that found in [12] and consists simply of detecting when patterns cause misclassification. These will be both patterns near decision boundaries in the final stages of optimization and those that may be further away in the early phase of optimization. In hyperspectral applications, we typically encounter data that is highly mixed, so we opt for a practical solution that can be implemented online, recognizing that even as we may accelerate convergence of an algorithm, we may still need to revisit patterns that are error-prone more than once. Thus, in our algorithm, we define a resampling buffer that will be part of the total input stream along with the regular data stream of images or regions of interest that comprise the training set. Entry into the resampling buffer is determined online as each pattern is processed, a category response determined, and updates performed. We call this approach *adaptive resampling of error-prone exemplars* (ARESEPE). The overall schema of ARESEPE is depicted in Fig. 1; it shows that an input controller samples from the original input data stream (potentially images, regions of interest, spectral libraries, etc.) and a resampling buffer, where patterns that have caused misclassification are placed with a probability proportional to their degree of misclassification. The latter criterion is made more precise in the next subsection. The input controller also serves to toggle the appropriate ground truth source, either associated with the original stream or the resampling buffer, so that samples and their labels remain aligned. The dashed lines from the two ground truth sources are used to portray the fact that this information is used for updating the classifier based on the training data in a general supervised

TABLE I

(1) *Phragmites australis* (Common Reed)	(2) *Spartina alterniflora* (Smooth Cordgrass)
(3) *Spartina patens (Salt-Hay)*	(4) *Salicornia virginica* (Perrenial Glasswort)
(5) *Borrichia frutescens (Sea Ox-eye)*	(6) *Juncus roemerianus* (Needle Rush)
(7) Water	(8) *Distichlis spicata (Saltgrass)*
(9) *Scirpus spp.* (Saltmarsh Bulrush)	(10) "Wrack"
(11) Mudflat/saltflat	(12) *Ammophila breviligulata* (American Beachgrass)
(13) Beach/sand	(14) *Uniola paniculata* (Sea-oats)
(15) Andropogon spp. (Broomsedge)	(16) *Myrica cerifera* (Bayberry)-dominated Thicket
(17) Pine/hardwood complex	(18) Peat Outcrop
(19) *Iva frutescens* (Marsh-elder)	

learning scenario. "X"s indicate where a probabilistic gating takes place; for example, samples from the input stream enter the resampling buffer based on a probability proportional to the degree of misclassification. The same choice is applied simultaneously at the ground truth resampling buffer to maintain synchronization of data and labels. The user defines rates for the two input sources, original stream and resampling buffer, and the size of the buffer itself. To date in all of the applications to which we have applied ARESEPE, a modest buffer serves adequately. The buffer is implemented as a first-in-first-out (FIFO) stack, but the input controller chooses samples from both the original input stream and the resampling buffer stochastically with rates of r_{buffer} and r_{stream} respectively. In Section IV, we explore the impact of independently varying the buffer size and r_{buffer}.

B. Buffer Entry Criterion: Minimum Misclassification Error

We have stated that the buffer entry criterion should be determined by the degree of misclassification that occurs. Patterns that do not produce error should not enter the buffer, while those that cause the most error should be the most likely to enter the resampling buffer. Notice that this criterion is more general than those mentioned earlier because it omits discussion of where the patterns must be located at different points in the evolution of the classifier optimization. Indeed, in the Results Section, we will see that the spatial distribution of erroneous patterns in the buffer does change during the optimization procedure. Our approach uses a misclassification measure first defined by Juang and Katagiri [10] as an alternative cost function for least mean square (LMS) error stochastic optimization. They observed that the goal of modeling is actually to minimize misclassification error, not the total error between target values and discriminant functions over all categories (LMS error). For discrete classification problems, though closely related, LMS error and misclassification error are not identical, i.e., multiple values of LMS error derived from different models for a specific pattern may map to the same answer (misclassification or correct classification). For a two-class problem, they noted that the natural measure for degree of misclassification was simply the difference between the individual discriminant functions, i.e., just the Bayesian *posterior* probabilities

$$d(\vec{x}) = P(C1 \mid \vec{x}) - P(C0 \mid \vec{x}). \tag{1}$$

To extend this to multiclass problems and maintain the idea of a continuously varying function that could be used in stochastic optimization, they defined an M-category discriminant function

$$d(\vec{x}) = -f_i + \left[\frac{1}{M-1}\sum_{j,j\neq i} f_j(\vec{x})^{\nu}\right]^{1/\nu} \tag{2}$$

where index i is the true category associated with input sample vector $\vec{x}$. The asymptotic limit as $\nu \to \infty$ is just

$$d_{\infty}(\vec{x}) = f_{\max} - f_i \tag{3}$$

where $f_{\max}$ is the maximum responding discriminant function not equal to the true discriminant function. Thus, a positive value of $d_{\infty}(\vec{x})$ represents the amount by which the winning discriminant function was larger than the true discriminant function.

While originally formulated as an alternative cost function for stochastic optimization of neural networks, the asymptotic minimum misclassification error measure defined in (3) provides a useful measure of the degree of misclassification that fulfills our need for a resampling buffer entry criterion. As patterns are presented alternately from the resampling buffer and the original input data stream (training set), whenever a pattern originates from the original data stream, we compute (3). If we calculate, the quantity

$$d_j = f_j - f_i \tag{4}$$

for each category node j, where as before, i is the index of the true category, and then compute $d_{\max}$

$$d_{\max} = \max_j d_j = d_{\infty}(\vec{x}) \tag{5}$$

then the sign of $d_{\max}$ will tell us whether the pattern was misclassified and will automatically determine the quantity d_{∞}. If a pattern is misclassified, we make the probability of entering the resampling buffer $\propto d_{\max}$. Note that $d_{\max} \in [-1, 1]$ if our discriminant functions satisfy the condition $f_i \in [0, 1]$. Our software implementation software [1] also includes a baseline acceptance probability. The acceptance probability is thus

$$P_{\text{accept}} = \theta(d_{\max})\Big(P_{\text{baseline prob}} + \left(\frac{d_{\max}}{\text{scale}}\right) * (1 - P_{\text{baseline prob}})\Big) \tag{6}$$

where θ is the Heaviside function (step function). In this equation, scale is usually set to 1, so that the probability of accep-

TABLE II
TRAINING SET. PERCENTAGE ACCURACY VERSUS UPDATES(SAMPLES) BPCE, $P_{\text{baseline prob}} = 0.5$, Buffer Size = 3600

Training Set: % Accuracy vs Updates(Samples) BPCE, $P_{baseline\ prob}$ = 0.5, Buffer Size = 3600							
	Varying r_{buffer}:						
Updates	0.0	0.1	0.25	0.35	0.5	0.75	0.9
0.0e+00	6.39 ± 5.06	6.54 ± 4.40	7.26 ± 4.68	4.18 ± 3.52	6.53 ± 5.13	4.68 ± 4.11	5.36 ± 4.66
5.0e+04	5.58 ± 4.38	4.20 ± 2.77	12.17 ± 7.35	14.56 ± 8.75	19.01 ± 10.99	30.63 ± 8.54	39.38 ± 6.87
1.0e+05	7.76 ± 4.50	9.58 ± 4.76	20.99 ± 7.35	27.02 ± 7.48	28.09 ± 11.23	45.22 ± 6.24	49.76 ± 6.33
2.5e+05	14.15 ± 7.26	27.32 ± 10.09	37.61 ± 5.49	44.67 ± 6.31	47.39 ± 8.75	65.36 ± 6.16	68.44 ± 4.21
5.0e+05	27.44 ± 5.84	38.56 ± 6.29	44.80 ± 9.26	53.00 ± 5.55	63.21 ± 9.83	75.17 ± 4.95	80.45 ± 3.29
7.5e+05	33.78 ± 7.39	39.71 ± 7.36	54.56 ± 6.30	65.48 ± 11.47	73.70 ± 4.92	81.10 ± 2.70	86.32 ± 2.16
1.0e+06	32.77 ± 8.61	45.81 ± 4.23	63.16 ± 6.50	71.78 ± 6.99	79.94 ± 3.13	85.37 ± 2.43	88.29 ± 2.82
2.5e+06	38.68 ± 4.61	57.31 ± 7.63	80.92 ± 2.79	86.13 ± 4.49	90.12 ± 2.06	95.07 ± 1.45	97.05 ± 0.46
5.0e+06	43.15 ± 10.01	75.04 ± 7.28	89.88 ± 2.18	94.47 ± 1.77	96.30 ± 1.43	98.82 ± 0.32	99.30 ± 0.38
7.5e+06	46.50 ± 9.59	79.07 ± 5.02	95.76 ± 1.22	97.13 ± 0.86	98.56 ± 0.71	99.57 ± 0.23	99.77 ± 0.11
1.0e+07	52.98 ± 6.33	84.18 ± 4.07	97.64 ± 1.00	98.65 ± 0.71	99.30 ± 0.37	99.81 ± 0.06	99.84 ± 0.07
2.5e+07	63.85 ± 8.84	97.71 ± 1.08	99.72 ± 0.15	99.83 ± 0.07	99.87 ± 0.05	99.89 ± 0.03	99.89 ± 0.04
5.0e+07	70.72 ± 7.59	99.71 ± 0.14	99.86 ± 0.04	99.88 ± 0.03	99.90 ± 0.03	99.90 ± 0.03	99.89 ± 0.04
1.0e+08	79.86 ± 7.45	99.90 ± 0.02	99.90 ± 0.03	99.89 ± 0.02	99.91 ± 0.03	99.90 ± 0.04	99.89 ± 0.04
1.2e+08	79.60 ± 7.28	99.90 ± 0.03	99.90 ± 0.03	99.90 ± 0.03	99.90 ± 0.03	99.90 ± 0.03	99.90 ± 0.04

TABLE III
CROSS-VALIDATION SET. PERCENTAGE ACCURACY VERSUS UPDATES(SAMPLES) BPCE, $P_{\text{baseline prob}} = 0.5$, Buffer Size = 3600

Cross-Validation Set: % Accuracy vs Updates(Samples) BPCE, $P_{baseline\ prob}$ = 0.5, Buffer Size = 3600							
	Varying r_{buffer}:						
Updates	0.0	0.1	0.25	0.35	0.5	0.75	0.9
0.0e+00	8.60 ± 10.77	5.12 ± 4.75	7.46 ± 8.48	2.62 ± 2.90	10.24 ± 12.20	3.49 ± 3.21	4.74 ± 8.09
5.0e+04	3.53 ± 4.22	4.10 ± 4.62	16.78 ± 15.29	17.95 ± 13.06	21.95 ± 15.35	35.84 ± 10.21	50.03 ± 6.09
1.0e+05	7.39 ± 7.39	12.13 ± 10.98	26.96 ± 14.27	33.70 ± 15.29	35.63 ± 17.06	53.18 ± 5.37	56.06 ± 7.36
2.5e+05	18.54 ± 13.25	34.16 ± 17.90	46.72 ± 10.04	49.52 ± 13.39	52.38 ± 10.16	65.14 ± 4.29	66.71 ± 5.79
5.0e+05	37.60 ± 10.41	46.35 ± 6.76	52.99 ± 10.81	57.48 ± 4.11	63.91 ± 7.93	70.79 ± 2.97	73.16 ± 2.72
7.5e+05	41.02 ± 12.30	48.44 ± 7.97	58.84 ± 5.16	66.26 ± 9.33	67.96 ± 3.27	74.03 ± 3.01	75.91 ± 1.75
1.0e+06	41.98 ± 12.11	52.67 ± 2.66	65.00 ± 4.84	67.23 ± 4.69	71.93 ± 2.16	76.37 ± 2.14	76.29 ± 2.09
2.5e+06	49.80 ± 6.66	62.74 ± 6.74	72.81 ± 3.18	75.04 ± 3.55	77.07 ± 2.24	79.21 ± 1.63	78.46 ± 2.54
5.0e+06	48.46 ± 8.35	69.84 ± 5.29	77.19 ± 2.82	77.07 ± 1.14	78.84 ± 1.50	80.15 ± 1.15	78.45 ± 1.63
7.5e+06	53.32 ± 8.23	73.24 ± 3.41	78.99 ± 1.62	78.21 ± 2.68	78.71 ± 2.24	79.52 ± 1.69	78.65 ± 1.92
1.0e+07	56.37 ± 5.29	74.27 ± 2.55	79.69 ± 1.44	79.30 ± 1.96	79.42 ± 1.50	80.11 ± 1.42	78.85 ± 1.89
2.5e+07	65.83 ± 8.18	79.64 ± 1.62	80.70 ± 1.19	80.34 ± 1.41	79.90 ± 1.00	79.89 ± 1.09	79.35 ± 1.50
5.0e+07	68.42 ± 4.31	80.81 ± 1.18	81.21 ± 0.81	80.69 ± 1.29	79.89 ± 1.04	80.18 ± 1.24	79.49 ± 1.35
1.0e+08	74.43 ± 5.40	81.48 ± 1.10	81.26 ± 0.67	80.97 ± 0.88	80.19 ± 1.10	80.33 ± 1.14	79.76 ± 1.40
1.2e+08	73.39 ± 7.13	81.24 ± 1.10	81.23 ± 0.73	80.93 ± 0.97	80.08 ± 0.99	80.42 ± 1.16	79.91 ± 1.37

tance is $\in [P_{\text{baseline prob}}, 1]$; however, it can be used to set an upper limit on acceptance probability.

III. EXAMPLE: PROBE2 AIRBORNE HYPERSPECTRAL IMAGERY

To illustrate ARESEPE, we have chosen a set of airborne hyperspectral data drawn from a larger scale study described in [2] and [3]. In particular, we evaluate land-cover classification models derived from a PROBE2 scene acquired on October 18, 2001 of Smith Island, VA, a barrier island in The Nature Conservancy's Virginia Coast Reserve (VCR).[1] Land-cover modeling using a HyMAP scene of this island from May 2000 was described in [2], while [3] addresses multiseason models that have been derived for this island and which show improvement over single-season models, including the set used for illustration in this paper. The database of labeled spectral samples was divided into a Training Set (3632 samples), a Cross-Validation Test Set (1971 samples) used to determine the best model during the optimization, and a Sequestered Test Set (2834 samples) that served as an independent test of generalization capability.

A. Ground Truth for Smith Island Land-Cover

Ground truth data used to validate the accuracy of these models is based on extensive ongoing ground surveys with global positioning system (GPS) and differential GPS (DGPS) carried out on Smith Island, VA (see [2] and [3]). The Smith Island scene was acquired at 4.5-m resolution with 124 spectral channels, ranging from 440-2486 nm. Scene dimensions are approximately 12.2 km × 2.5 km. To obtain reflectance data, the 6S algorithm described in [8] was applied to the radiance data, which was then polished using the EFFORT [4] algorithm. In the present study, a database of spectral samples from the 19 categories listed in Table I were extracted from the October PROBE2 scene within areas delimited by the GPS and DGPS

[1]Web Site for the University of Virginia's Long Term Ecological Research Program. See http://www.vcrlter.virginia.edu.

TABLE IV
SEQUESTERED TEST. PERCENTAGE ACCURACY VERSUS UPDATES(SAMPLES) BPCE, $P_{\text{baseline prob}} = 0.5$, Buffer Size = 3600

Sequestered Test: % Accuracy vs Updates(Samples) BPCE, $P_{baseline\ prob}$ = 0.5, Buffer Size = 3600							
	Varying r_{buffer}:						
Updates	0.0	0.1	0.25	0.35	0.5	0.75	0.9
0.0e+00	7.15 ± 6.16	4.52 ± 2.97	5.87 ± 4.48	4.74 ± 3.22	5.87 ± 4.48	4.61 ± 4.71	5.31 ± 4.37
5.0e+04	4.16 ± 3.21	4.89 ± 4.74	12.11 ± 9.31	14.80 ± 9.28	12.11 ± 9.31	27.91 ± 7.35	33.85 ± 5.30
1.0e+05	7.42 ± 4.60	9.47 ± 8.38	19.81 ± 7.45	24.93 ± 9.24	19.81 ± 7.45	38.37 ± 4.51	42.19 ± 4.59
2.5e+05	16.07 ± 7.58	25.30 ± 11.58	33.89 ± 4.06	35.90 ± 6.35	33.89 ± 4.06	49.34 ± 6.26	52.63 ± 5.15
5.0e+05	28.24 ± 5.22	35.17 ± 4.14	40.12 ± 6.92	41.63 ± 3.63	40.12 ± 6.92	56.68 ± 4.41	60.77 ± 3.06
7.5e+05	31.14 ± 6.37	37.75 ± 6.54	43.65 ± 3.82	50.57 ± 8.14	43.65 ± 3.82	62.29 ± 2.40	63.72 ± 1.27
1.0e+06	33.12 ± 7.53	40.68 ± 3.23	48.52 ± 4.90	56.12 ± 5.47	48.52 ± 4.90	64.18 ± 2.47	64.72 ± 1.15
2.5e+06	36.14 ± 2.43	48.05 ± 5.30	61.64 ± 2.97	63.37 ± 2.37	61.64 ± 2.97	67.71 ± 1.51	67.18 ± 1.84
5.0e+06	38.77 ± 5.68	60.03 ± 5.57	65.11 ± 2.75	67.58 ± 2.40	65.11 ± 2.75	68.32 ± 1.59	68.00 ± 1.26
7.5e+06	43.21 ± 5.06	61.73 ± 3.96	68.68 ± 1.83	67.50 ± 1.61	68.68 ± 1.83	67.78 ± 1.14	68.27 ± 1.21
1.0e+07	46.37 ± 7.83	63.34 ± 3.04	68.32 ± 2.37	67.51 ± 1.25	68.32 ± 2.37	68.03 ± 1.47	68.06 ± 0.94
2.5e+07	52.77 ± 6.29	68.43 ± 1.69	69.45 ± 1.85	68.52 ± 1.38	69.45 ± 1.85	68.61 ± 1.64	68.57 ± 1.28
5.0e+07	57.05 ± 3.79	69.53 ± 1.07	69.71 ± 0.91	69.08 ± 1.76	69.71 ± 0.91	68.88 ± 1.85	68.79 ± 1.27
1.0e+08	62.91 ± 4.13	70.29 ± 1.47	70.04 ± 1.41	69.39 ± 1.69	70.04 ± 1.41	69.06 ± 1.54	68.99 ± 1.35
1.2e+08	63.36 ± 4.26	70.52 ± 1.63	70.24 ± 1.36	69.45 ± 1.56	70.06 ± 1.13	69.18 ± 1.68	69.08 ± 1.36

TABLE V
TRAINING SET. PERCENTAGE ACCURACY VERSUS UPDATES(SAMPLES) BPLMS, $P_{\text{baseline prob}} = 0.5$, Buffer Size = 3600

Training Set: % Accuracy vs Updates(Samples) BPLMS, $P_{baseline\ prob}$ = 0.5, Buffer Size = 3600					
	Varying r_{buffer}:				
Updates	0.0	0.25	0.35	0.5	0.9
0.0e+00	5.45 ± 4.91	6.52 ± 4.27	3.77 ± 3.45	7.34 ± 4.77	4.61 ± 3.98
5.0e+04	9.54 ± 3.62	8.50 ± 3.35	10.05 ± 1.40	7.53 ± 3.92	8.03 ± 5.54
1.0e+05	8.60 ± 3.16	7.82 ± 4.71	6.34 ± 4.21	6.49 ± 4.77	13.77 ± 10.34
2.5e+05	10.48 ± 3.45	8.42 ± 2.82	12.12 ± 6.92	9.85 ± 3.15	24.81 ± 6.27
5.0e+05	14.00 ± 4.29	19.90 ± 9.34	17.15 ± 5.84	19.69 ± 4.18	41.03 ± 7.44
7.5e+05	21.78 ± 8.58	30.00 ± 7.95	31.45 ± 9.35	25.47 ± 8.20	46.33 ± 9.35
1.0e+06	29.01 ± 5.22	35.76 ± 7.09	36.03 ± 7.02	36.33 ± 11.74	52.60 ± 5.75
2.5e+06	43.00 ± 4.71	49.48 ± 4.36	51.92 ± 7.60	58.90 ± 6.35	73.27 ± 2.81
5.0e+06	47.91 ± 4.55	64.38 ± 5.44	68.09 ± 8.76	75.55 ± 3.79	87.53 ± 2.02
7.5e+06	56.90 ± 5.54	75.57 ± 2.98	76.04 ± 5.73	84.55 ± 4.74	93.87 ± 0.96
1.0e+07	59.09 ± 5.61	79.60 ± 5.65	83.12 ± 4.06	88.36 ± 2.29	96.88 ± 0.59
2.5e+07	72.24 ± 3.38	91.37 ± 3.22	97.46 ± 1.03	99.01 ± 0.61	99.85 ± 0.03
5.0e+07	79.61 ± 3.52	99.53 ± 0.27	99.75 ± 0.14	99.85 ± 0.06	99.91 ± 0.03
1.0e+08	84.78 ± 3.28	99.89 ± 0.05	99.89 ± 0.03	99.90 ± 0.04	99.91 ± 0.03
1.2e+08	87.89 ± 1.87	99.90 ± 0.04	99.88 ± 0.03	99.89 ± 0.04	99.92 ± 0.03

ground survey. The categories range from specific plant species to vegetation communities (for species that do not appear in monotypic stands) and cover the majority of the principal wetland, dune, and upland vegetation and related ground cover types. Further data and ground truth details are in [2] and [3].

IV. RESULTS

In order to illustrate ARESEPE, we chose a popular neural network algorithm, the backward propagation (BP) algorithm [14]. Two different BP cost functions were evaluated: one using cross-entropy (BPCE) [13], and the other the least mean square (BPLMS) error [14]. The primary control parameters associated with ARESEPE were varied, and performance was compared against BPLMS and BPCE without ARESEPE. Tables II–IV (BPCE) and Tables V–VII (BPLMS) show that the convergence rate of the overall accuracy is improved steadily as r_{buffer} is increased ($r_{\text{buffer}} = 0.0$ is without ARESEPE) for the Training, Cross-Validation, and Sequestered Test sets.

Although, performance was measured for each set every 50 000 samples (updates), the tables show only a set of highlighted points, since trials were run to 1.2×10^8 updates. The tables portray the mean and standard deviation of the total accuracy over all pixels for the 19 categories in Table I; ten trials were performed for each parameter setting listed. Notice that the convergence rates steadily improve up to about $r_{\text{buffer}} = 0.90$. Beyond that convergence improvements level off. Full convergence curves (mean and error bars portraying the standard deviation) are shown in Fig. 2 for BPLMS and BPCE with ARESEPE at $r_{\text{buffer}} = 0.90$ and without ARESEPE ($r_{\text{buffer}} = 0.0$).

Notice that the asymptotic portion of the curve for the Sequestered Test Set is reached around 1×10^6 samples for BPCE at $r_{\text{buffer}} = 0.9$, while the same level of expected performance is still not achieved even at 1×10^8 samples when ARESEPE is not used. Thus, convergence rate has been accelerated by more than a factor of 100 (20 db) using ARESEPE. Also note that BPLMS with ARESEPE always converges more slowly

TABLE VI
CROSS-VALIDATION SET PERCENTAGE ACCURACY VERSUS UPDATES(SAMPLES) BPLMS, $P_{\text{baseline prob}} = 0.5$, Buffer Size $= 3600$

Cross-Validation Set: % Accuracy vs Updates(Samples) BPLMS, $P_{baseline\ prob}$ = 0.5, Buffer Size = 3600					
	Varying r_{buffer}:				
Updates	0.0	0.25	0.35	0.5	0.9
0.0e+00	5.05 ± 8.18	7.45 ± 8.42	4.40 ± 4.90	7.92 ± 8.32	2.72 ± 3.56
5.0e+04	11.98 ± 9.00	8.19 ± 4.15	9.93 ± 2.72	6.40 ± 4.75	7.39 ± 7.87
1.0e+05	10.43 ± 7.27	7.67 ± 8.05	7.88 ± 8.76	5.40 ± 5.19	15.60 ± 15.11
2.5e+05	11.79 ± 7.72	6.22 ± 4.40	12.58 ± 12.23	8.76 ± 4.70	28.19 ± 11.03
5.0e+05	14.57 ± 9.33	21.14 ± 15.30	17.16 ± 4.76	16.54 ± 8.60	49.31 ± 10.35
7.5e+05	24.14 ± 15.61	34.80 ± 16.59	38.52 ± 15.42	25.16 ± 12.43	49.90 ± 12.25
1.0e+06	36.85 ± 9.86	46.77 ± 7.90	40.86 ± 11.83	42.66 ± 15.11	56.08 ± 6.46
2.5e+06	50.78 ± 9.41	50.49 ± 8.27	55.85 ± 7.98	59.07 ± 8.13	70.46 ± 2.38
5.0e+06	57.26 ± 4.80	62.85 ± 6.20	67.85 ± 4.82	71.43 ± 2.92	77.44 ± 1.69
7.5e+06	60.35 ± 4.31	72.58 ± 3.24	69.86 ± 5.76	74.22 ± 2.98	77.63 ± 1.62
1.0e+07	61.45 ± 5.37	72.90 ± 3.15	76.23 ± 2.80	78.15 ± 2.26	78.45 ± 1.85
2.5e+07	71.33 ± 3.54	78.13 ± 2.31	80.14 ± 1.40	81.68 ± 1.73	79.48 ± 1.52
5.0e+07	75.68 ± 2.94	81.16 ± 0.76	81.67 ± 0.82	81.55 ± 1.18	80.05 ± 0.83
1.0e+08	76.51 ± 1.87	81.32 ± 0.58	81.10 ± 0.74	82.01 ± 1.18	80.49 ± 0.82
1.2e+08	77.71 ± 2.28	81.41 ± 0.45	81.14 ± 0.77	81.90 ± 1.18	80.56 ± 0.78

TABLE VII
SEQUESTERED TEST. PERCENTAGE ACCURACY VERSUS UPDATES(SAMPLES) BPLMS, $P_{\text{baseline prob}} = 0.5$, Buffer Size $= 3600$

Sequestered Test Set: % Accuracy vs Updates(Samples) BPLMS, $P_{baseline\ prob}$ = 0.5, Buffer Size = 3600					
	Varying r_{buffer}:				
Updates	0.0	0.25	0.35	0.5	0.9
0.0e+00	4.58 ± 4.45	6.30 ± 5.30	4.85 ± 4.93	5.90 ± 4.52	4.05 ± 4.81
5.0e+04	8.90 ± 3.52	6.98 ± 2.52	7.84 ± 1.31	6.27 ± 4.45	6.64 ± 5.58
1.0e+05	7.23 ± 3.69	7.41 ± 5.25	5.58 ± 4.59	4.81 ± 3.45	11.42 ± 9.58
2.5e+05	8.84 ± 4.66	7.01 ± 2.41	10.42 ± 6.96	8.36 ± 1.94	20.68 ± 5.67
5.0e+05	11.84 ± 4.53	18.12 ± 9.54	14.39 ± 5.74	16.08 ± 5.12	36.48 ± 6.32
7.5e+05	19.88 ± 8.68	27.47 ± 10.81	27.29 ± 9.60	21.85 ± 9.45	38.03 ± 6.57
1.0e+06	27.56 ± 7.86	34.84 ± 7.80	32.80 ± 5.64	32.22 ± 9.80	42.23 ± 4.24
2.5e+06	36.48 ± 5.30	40.36 ± 4.26	41.53 ± 3.80	47.31 ± 7.27	54.90 ± 3.48
5.0e+06	41.86 ± 4.94	52.17 ± 6.79	53.46 ± 5.39	58.26 ± 2.97	65.80 ± 2.10
7.5e+06	47.45 ± 4.52	60.12 ± 3.32	58.82 ± 4.12	63.89 ± 3.77	67.97 ± 1.27
1.0e+07	47.46 ± 6.07	62.30 ± 3.29	64.12 ± 2.47	66.91 ± 2.58	68.66 ± 0.87
2.5e+07	58.81 ± 3.32	67.15 ± 2.28	69.07 ± 1.22	69.76 ± 1.64	68.45 ± 1.02
5.0e+07	62.78 ± 4.47	69.11 ± 0.96	69.49 ± 0.68	69.64 ± 1.21	68.88 ± 1.34
1.0e+08	64.61 ± 2.78	69.46 ± 1.14	69.72 ± 1.06	69.80 ± 1.05	69.36 ± 1.44
1.2e+08	66.51 ± 2.30	69.57 ± 1.10	69.63 ± 0.99	69.90 ± 1.17	69.38 ± 1.51

than BPCE with ARESEPE (Tables II–IV, Tables V–VII, and Fig. 2), except at $r_{\text{buffer}} = 0.0$ (without ARESEPE) where the BPCE curve initially rises faster, and then converges marginally more slowly in the asymptotic portion of the curves. When ARESEPE is used, the faster convergence of BPCE compared to BPLMS is probably due to the fact that BPCE spends less time in the vicinity of local minima than BPLMS, owing to the form of the gradient used in the stochastic gradient descent [2], [3], [13]. Note that most commercial packages such as ENVI [5] use BPLMS without ARESEPE in their neural network implementation.

The buffer size was also varied, revealing that there were two distinctly different ranges of buffer sizes that worked well. Tables VIII–X show accuracies at $r_{\text{buffer}} = 0.5$ for varying buffer sizes as a function of the number of updates. When the buffer size was between 2500–3600 samples, this was optimal. Likewise, convergence rate was nearly as good for a buffer size of 625 samples. In the former case, the buffer size is large enough to represent all possible errors, while a size of 625 was comparable to the number of distinct, erroneous patterns when the distribution of the buffer was probed in the early stages of training. The small buffer is more agile (due to its FIFO nature) than buffer sizes of 1600 samples; likewise, success is achieved at buffer sizes of 2500–3600, because the buffer readily encompasses all possible sources of error.

We also examined the distribution of pixels in the resampling buffer to understand its evolution. Overall, we found that it progressively includes a greater percentage of boundary pixels as time (number of updates) increases. Fig. 3 shows two regions derived from the PROBE2 scene (Fig. 4). DGPS ground-surveyed regions of interest (ROIs) used in the study are highlighted as colored lines, and the contents of the resampling buffer are shown in the early and late stages of training. Fig. 3 shows that although core pixels exist in the buffer at both early and later times, a much large percentage of boundary pixels occurs at later times as the model attempts to refine the decision

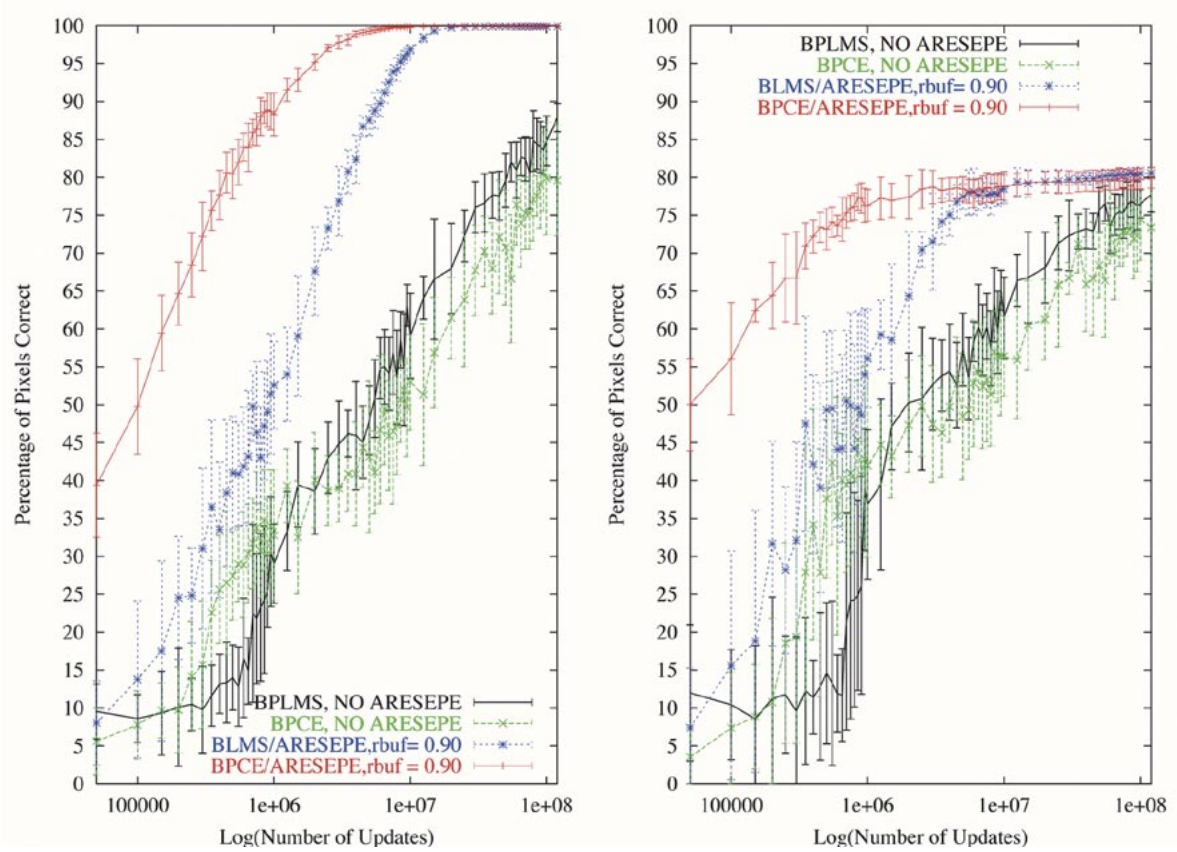

(a) (b)

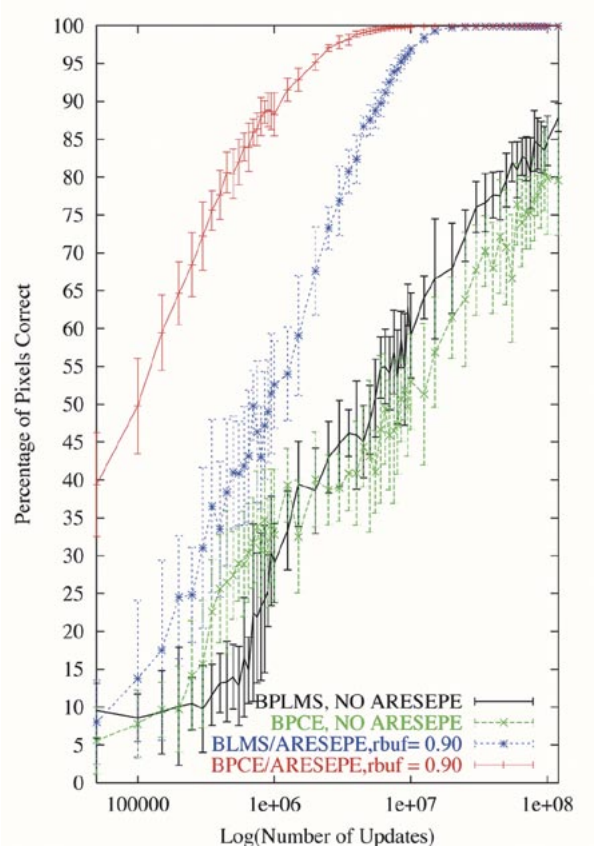

(c)

Fig. 2. Percentage correct versus log (number of updates) for (a) training, (b) cross-validation test, and (c) sequestered test sets. (Shown) BPLMS with and without ARESEPE and BPCE with and without ARESEPE. ARESEPE curves are for $r_{\text{buffer}} = 0.90$. BPCE with ARESEPE achieves two orders of magnitude improvement in convergence rate compared to both BPCE and BPLMS without ARESEPE.

TABLE VIII
TRAINING SET. PERCENTAGE ACCURACY VERSUS UPDATES(SAMPLES) BPCE, $P_{\text{baseline prob}} = 0.5, r_{\text{buffer}} = 0.5$

Training Set: % Accuracy vs Updates(Samples) BPCE, $P_{baseline\ prob} = 0.5, r_{buffer} = 0.5$								
	Varying Buffer Size (No. of Samples)							
Updates	25	100	225	400	625	1600	2500	3600
0.0e+00	3.78 ± 3.68	5.84 ± 4.47	5.31 ± 3.47	4.58 ± 3.47	5.55 ± 3.58	5.19 ± 5.32	7.08 ± 3.76	6.53 ± 5.13
5.0e+04	8.65 ± 2.68	9.52 ± 4.89	17.63 ± 10.50	17.81 ± 7.92	20.29 ± 8.53	15.38 ± 6.90	19.66 ± 7.43	19.01 ± 10.99
1.0e+05	6.75 ± 4.42	15.71 ± 9.53	26.64 ± 10.52	30.32 ± 7.27	38.33 ± 8.77	24.43 ± 9.18	34.51 ± 8.51	28.09 ± 11.23
2.5e+05	15.55 ± 8.69	26.92 ± 8.63	34.03 ± 4.85	38.88 ± 10.28	43.80 ± 6.92	35.65 ± 7.73	44.82 ± 7.07	47.39 ± 8.75
5.0e+05	27.78 ± 6.26	35.21 ± 3.49	41.70 ± 7.49	47.37 ± 7.29	57.38 ± 8.02	44.96 ± 5.62	65.06 ± 5.06	63.21 ± 9.83
7.5e+05	28.96 ± 4.82	39.38 ± 4.99	39.35 ± 5.29	60.82 ± 10.16	69.56 ± 6.70	52.65 ± 5.49	73.16 ± 5.17	73.70 ± 4.92
1.0e+06	35.85 ± 4.06	37.92 ± 6.24	39.08 ± 10.54	68.09 ± 6.05	74.74 ± 6.35	54.62 ± 4.84	80.42 ± 2.44	79.94 ± 3.13
2.5e+06	44.04 ± 3.80	43.12 ± 5.28	66.88 ± 6.85	87.15 ± 3.49	91.37 ± 1.99	73.15 ± 4.04	90.45 ± 3.34	90.12 ± 2.06
5.0e+06	43.94 ± 8.48	57.14 ± 9.75	89.94 ± 2.82	96.60 ± 1.29	97.54 ± 1.51	83.41 ± 3.45	97.74 ± 1.10	96.30 ± 1.43
7.5e+06	50.02 ± 9.28	58.36 ± 15.15	96.08 ± 2.26	98.96 ± 0.58	99.20 ± 0.40	84.23 ± 3.63	98.97 ± 0.54	98.56 ± 0.71
1.0e+07	54.00 ± 6.59	65.50 ± 13.69	98.47 ± 1.02	99.58 ± 0.17	99.69 ± 0.12	86.77 ± 2.03	99.59 ± 0.21	99.30 ± 0.37
2.5e+07	63.62 ± 9.84	90.05 ± 9.23	99.81 ± 0.14	99.86 ± 0.06	99.88 ± 0.04	92.36 ± 1.86	99.87 ± 0.06	99.87 ± 0.05
5.0e+07	73.24 ± 10.13	99.29 ± 1.04	99.87 ± 0.04	99.87 ± 0.05	99.90 ± 0.02	94.56 ± 2.07	99.88 ± 0.04	99.90 ± 0.03
1.0e+08	81.02 ± 7.35	99.89 ± 0.04	99.86 ± 0.05	99.88 ± 0.05	99.91 ± 0.02	96.99 ± 1.53	99.89 ± 0.05	99.91 ± 0.03
1.2e+08	83.38 ± 11.11	99.89 ± 0.05	99.88 ± 0.04	99.90 ± 0.03	99.91 ± 0.02	97.94 ± 0.60	99.88 ± 0.05	99.90 ± 0.03

TABLE IX
CROSS-VALIDATION SET. PERCENTAGE ACCURACY VERSUS UPDATES(SAMPLES) BPCE/$P_{\text{baseline prob}} = 0.5, r_{\text{buffer}} = 0.5$

Cross-Validation Set: Accuracy vs Updates(Samples) BPCE/ $P_{baseline\ prob} = 0.5, r_{buffer} = 0.5$								
	Varying Buffer Size (No. of Samples)							
Updates	25	100	225	400	625	1600	2500	3600
0.0e+00	2.30 ± 3.61	5.24 ± 4.71	4.94 ± 4.21	3.19 ± 3.64	4.99 ± 4.62	6.34 ± 8.78	6.50 ± 5.08	10.24 ± 12.20
5.0e+04	8.75 ± 3.81	9.17 ± 4.79	21.05 ± 15.17	22.14 ± 15.27	22.80 ± 11.95	20.54 ± 11.16	25.64 ± 16.03	21.95 ± 15.35
1.0e+05	5.80 ± 8.47	15.14 ± 13.92	31.24 ± 15.10	36.04 ± 12.06	43.39 ± 10.50	32.02 ± 15.57	41.00 ± 13.83	35.63 ± 17.06
2.5e+05	19.03 ± 16.01	28.75 ± 14.26	43.20 ± 7.69	41.22 ± 12.77	45.42 ± 14.42	44.33 ± 13.59	46.20 ± 15.43	52.38 ± 10.16
5.0e+05	37.18 ± 6.74	40.58 ± 11.26	48.45 ± 6.96	45.12 ± 12.09	55.33 ± 8.75	50.85 ± 9.41	61.99 ± 4.78	63.91 ± 7.93
7.5e+05	36.53 ± 9.24	49.83 ± 5.27	43.38 ± 9.30	62.21 ± 8.46	66.65 ± 4.76	57.02 ± 3.63	68.04 ± 4.07	67.96 ± 3.27
1.0e+06	43.41 ± 4.74	49.42 ± 7.42	45.47 ± 11.71	65.93 ± 2.95	69.51 ± 6.42	58.26 ± 5.20	72.18 ± 3.61	71.93 ± 2.16
2.5e+06	52.83 ± 5.36	47.21 ± 8.20	64.16 ± 4.60	74.93 ± 2.56	77.06 ± 2.48	70.39 ± 3.21	75.60 ± 2.82	77.07 ± 2.24
5.0e+06	53.09 ± 5.92	63.81 ± 7.70	76.23 ± 3.61	78.73 ± 1.68	78.94 ± 2.32	75.01 ± 4.21	78.66 ± 1.00	78.84 ± 1.50
7.5e+06	54.62 ± 8.24	61.27 ± 9.84	77.86 ± 1.79	79.30 ± 1.32	79.15 ± 1.15	77.29 ± 2.62	78.91 ± 1.68	78.71 ± 2.24
1.0e+07	59.12 ± 5.24	67.05 ± 8.06	79.42 ± 1.31	79.63 ± 0.97	79.51 ± 0.86	78.13 ± 2.72	79.75 ± 1.29	79.42 ± 1.50
2.5e+07	62.64 ± 7.30	74.05 ± 5.93	80.31 ± 1.78	80.61 ± 1.45	80.05 ± 0.91	79.49 ± 1.82	80.52 ± 0.86	79.90 ± 1.00
5.0e+07	68.08 ± 7.41	80.20 ± 2.00	80.94 ± 1.34	81.11 ± 1.42	80.68 ± 1.19	80.08 ± 1.22	80.58 ± 0.84	79.89 ± 1.04
1.0e+08	71.59 ± 3.77	80.57 ± 1.37	81.15 ± 1.04	81.09 ± 1.48	80.97 ± 1.04	80.79 ± 1.29	80.84 ± 0.89	80.19 ± 1.10
1.2e+08	74.21 ± 5.23	80.64 ± 1.38	80.98 ± 1.09	81.14 ± 1.41	80.98 ± 0.91	81.53 ± 1.30	80.83 ± 0.85	80.08 ± 0.99

TABLE X
SEQUESTERED TEST SET. PERCENTAGE ACCURACY VERSUS UPDATES(SAMPLES) BPCE/$P_{\text{baseline prob}} = 0.5, r_{\text{buffer}} = 0.5$

Sequestered Test Set: Accuracy vs Updates(Samples) BPCE/ $P_{baseline\ prob} = 0.5, r_{buffer} = 0.5$								
	Varying Buffer Size (No. of Samples)							
Updates	25	100	225	400	625	1600	2500	3600
0.0e+00	2.90 ± 2.53	6.60 ± 4.46	5.62 ± 4.27	3.42 ± 2.61	7.00 ± 3.90	4.80 ± 4.96	5.44 ± 2.60	6.86 ± 6.09
5.0e+04	7.70 ± 3.66	7.87 ± 4.11	16.37 ± 10.08	15.80 ± 9.11	16.89 ± 6.55	18.25 ± 8.59	18.61 ± 7.71	17.73 ± 11.10
1.0e+05	5.07 ± 4.42	13.66 ± 9.21	23.57 ± 10.63	28.61 ± 8.16	32.18 ± 7.89	23.52 ± 9.19	30.52 ± 6.67	26.46 ± 10.42
2.5e+05	16.25 ± 11.54	24.35 ± 8.89	31.06 ± 5.28	33.20 ± 10.22	34.66 ± 7.85	34.60 ± 7.44	34.58 ± 6.86	39.77 ± 5.05
5.0e+05	27.63 ± 4.88	31.42 ± 6.36	35.79 ± 5.40	36.94 ± 5.53	45.20 ± 5.37	39.40 ± 6.80	50.60 ± 4.44	49.40 ± 6.89
7.5e+05	28.11 ± 5.59	35.31 ± 4.02	33.16 ± 3.82	47.60 ± 7.89	54.99 ± 6.50	44.74 ± 1.66	56.64 ± 3.23	56.39 ± 4.28
1.0e+06	32.63 ± 4.31	35.81 ± 3.77	35.38 ± 8.73	54.01 ± 3.55	58.30 ± 4.16	45.65 ± 3.95	61.11 ± 3.22	60.06 ± 2.35
2.5e+06	39.56 ± 4.88	38.45 ± 3.90	53.20 ± 5.71	64.61 ± 1.68	66.95 ± 1.77	58.47 ± 3.72	65.96 ± 2.26	66.35 ± 2.33
5.0e+06	41.78 ± 3.76	50.69 ± 7.48	65.80 ± 2.92	67.51 ± 1.90	67.65 ± 1.38	64.29 ± 2.85	67.03 ± 2.09	68.27 ± 0.97
7.5e+06	44.78 ± 8.41	49.03 ± 9.57	66.36 ± 2.98	68.46 ± 1.55	67.80 ± 1.52	65.76 ± 4.05	67.35 ± 2.05	69.01 ± 1.22
1.0e+07	47.05 ± 5.97	54.80 ± 8.39	68.12 ± 2.65	68.34 ± 1.45	68.61 ± 1.15	66.85 ± 1.39	68.28 ± 2.00	69.53 ± 0.67
2.5e+07	52.72 ± 6.91	64.40 ± 4.49	69.34 ± 1.53	69.45 ± 1.81	69.07 ± 1.21	69.88 ± 2.10	68.83 ± 1.72	69.70 ± 1.01
5.0e+07	57.70 ± 7.18	69.15 ± 2.43	69.64 ± 1.66	69.64 ± 1.55	69.53 ± 1.05	70.15 ± 1.18	69.10 ± 1.99	69.85 ± 0.86
1.0e+08	60.40 ± 5.68	68.84 ± 2.02	69.75 ± 1.97	69.68 ± 1.35	69.73 ± 1.25	70.58 ± 1.63	69.51 ± 1.69	69.88 ± 1.18
1.2e+08	62.76 ± 6.71	69.02 ± 1.54	69.52 ± 1.74	69.92 ± 1.40	69.53 ± 1.08	71.04 ± 0.86	69.31 ± 1.94	70.06 ± 1.13

boundaries. Likewise, the plots in Fig. 2 show that using ARESEPE significantly reduces the variance of the accuracy curves, especially in the later stages of optimization. This is another indication that ARESEPE is forcing the model to examine only

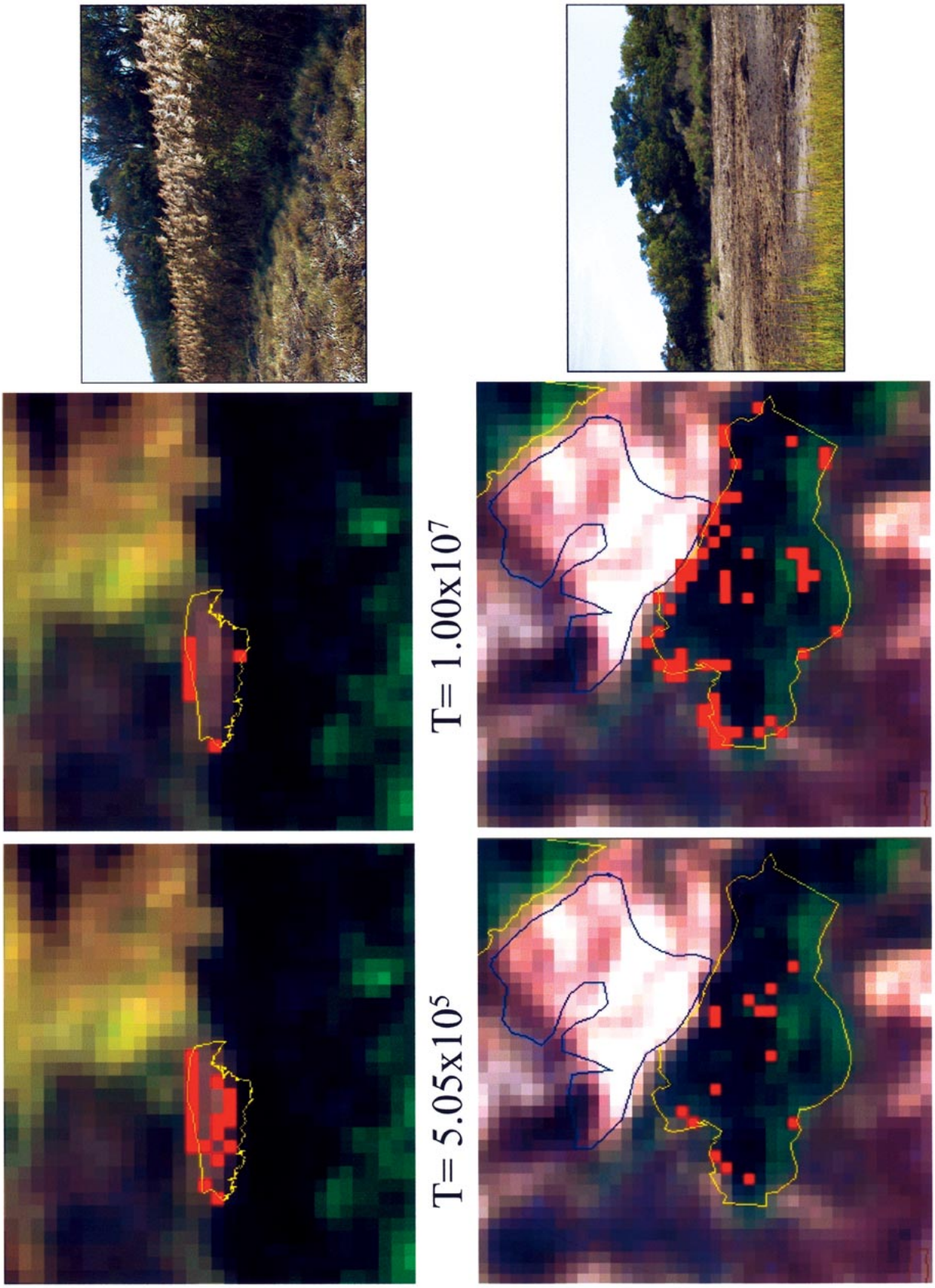

Fig. 3. Evolution of the ARESEPE resampling buffer contents. RGB images derived from PROBE2 for two regions in the study and shown during the early [(left) $t = 5.05 \times 10^5$] and late stages of training [(right) $t = 1 \times 10^7$ updates] with ARESEPE ($r_{\text{buffer}} = 0.9$). DGPS ground-surveyed ROIs are colored lines. Resampling buffer pixels are highlighted in red. As time increases, the percentage of boundary pixels increases. Also, the total number of distinct pixels across all surveyed ROIs in the resampling buffer increases from 432 points to 1046. (Top) *Phragmites australis* (Common Reed) ROI near *Myrica cerifera* thicket and brackish marsh grass *Distichlis spicata*. (Bottom) Pine-Hardwood Complex adjacent to a "wrack" zone.

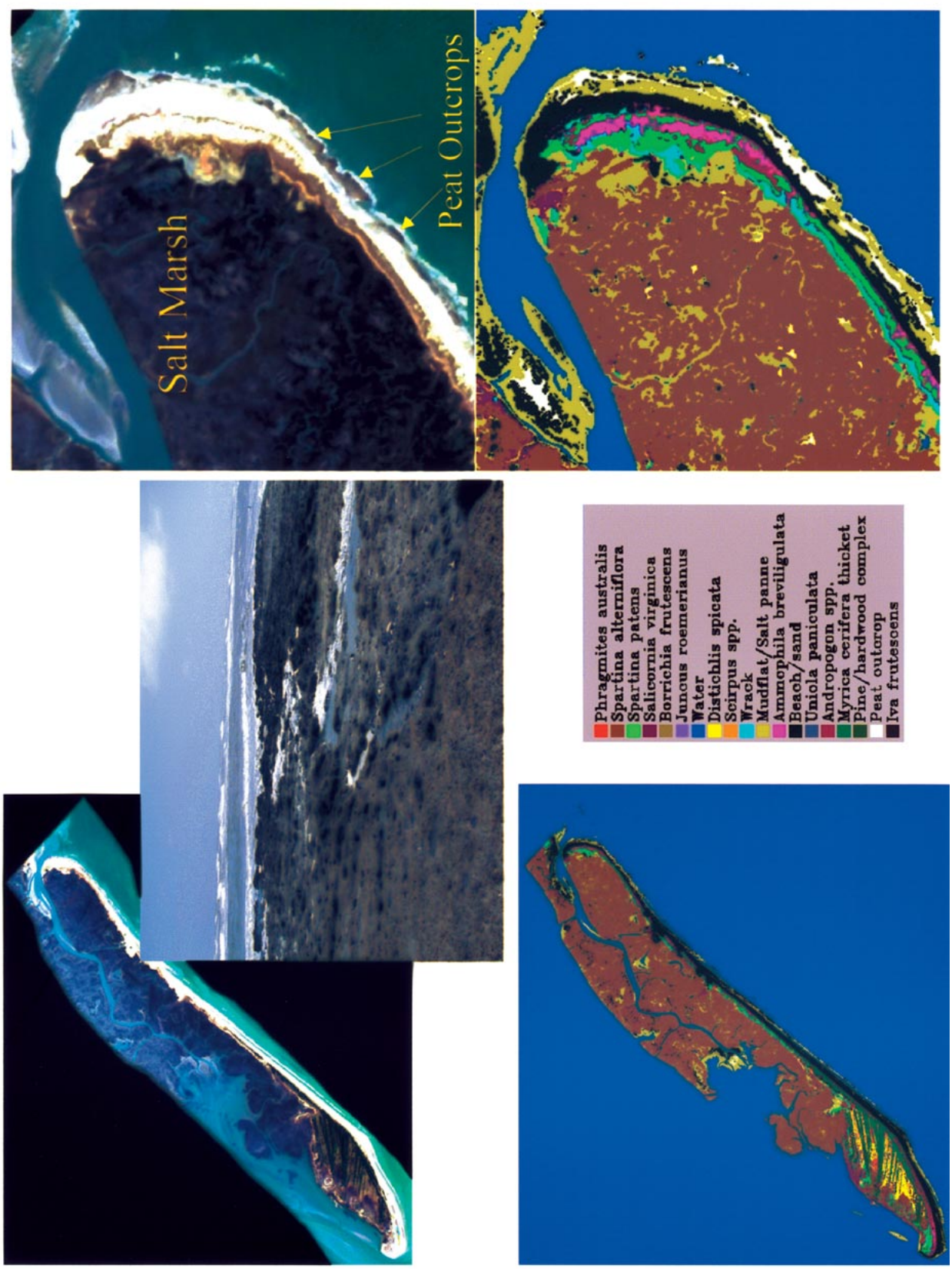

Fig. 4. (Upper left) PROBE2 scene of Smith Island, VA, from October 18, 2001 and (lower left) corresponding land-cover classification derived using BPCE with ARESEPE. (Enlargements) The northern end of the island and the corresponding land-cover classification. The photo inset from the northern end of the island shows typical peat outcrop. These are well delineated by the classification, as are dune and salt marsh vegetation species.

those patterns actually causing error near the boundaries, rather than distant patterns which might otherwise lead to larger changes in decision vectors and, thus, greater oscillation near the minimum. Thus, the properties of the ARESEPE resampling buffer are consistent with those originally recommended by Foody [6].

A typical land-cover classification obtained with BPCE and ARESEPE is shown in Fig. 4. This is the result of applying the model trained and tested using the PROBE2 spectra labeled from our ground surveys. After optimization, the model was applied to the entire scene to obtain the land-cover classification shown. Further details of these modeling efforts can be found in [2] and [3], both of which give more details about individual category accuracies. In the present work, we emphasize the convergence improvements that can be obtained using ARESEPE. In fact, using ARESEPE with $r_{\text{buffer}} = 0.9$ allowed us to reach the asymptotic region of the performance curves around $\sim 1 \times 10^6$ samples in roughly 12 min on an AMD Athlon XP 1800+. Although we terminated the experiments at $\sim 1.2 \times 10^8$ samples (updates), it clearly can be seen that waiting 100 times longer does not give us large improvements. Ultimately, we had to determine the time at which the benefits of additional performance increases were not worth the additional processing time; this is the notion of a "patience parameter." For us, this was $\sim$ 24 h; however, many real-world applications demand rapid response, and the ability to reach the asymptotic portion of the accuracy curve in under 12 min using ARESEPE versus 24 h without ARESEPE is thus a significant advantage.

V. Summary and Conclusion

We have demonstrated a completely general approach to accelerating the convergence rate of statistical classifiers. Although the approach was illustrated with popular neural network algorithms (BPLMS and BPCE), our new algorithm (ARESEPE) could be applied to any statistical classifier that uses stochastic optimization to obtain a model. Using BPCE with ARESEPE led to a two orders of magnitude improvement in convergence rate. The fact that ARESEPE is an online algorithm with minimal computational overhead and storage requirements allows us to apply the algorithm to high-dimensional datasets such as the PROBE2 data (which had 124 dimensions) used in this study. Most of the algorithms previously described were too inefficient to be applied to the large high-dimensional imagery databases that are found in hyperspectral applications. This has significant implications for many algorithms, and in particular for many commercially available software packages that use stochastic optimization techniques in their implementations of vector quantization, neural networks, and other statistical classifiers. ARESEPE works because it identifies error-prone patterns that should be revisited more frequently. In the latter stages of optimization, this is usually near the decision boundaries of the classifiers where errors are most likely, a fact which was confirmed by examining the contents of the resampling buffer. In addition to improving convergence rate, ARESEPE greatly reduced the variance of the accuracy curves, especially in the later stages of optimization. This is another indication that ARESEPE forces the model to examine only those patterns actually causing error near the boundaries. ARESEPE requires minimal overhead, a simple buffer that is resampled with a user-specified rate along with the original input data stream. Computational overhead is also minimal because the buffer entry criterion is based on a simple asymptotic formula for degree of misclassification. ARESEPE also represents an improvement over many of the previously described algorithms for active sampling because the resampling criterion (buffer entry criterion) only examines degree of misclassification; this also means that it will be more efficient in the early stages of optimization than algorithms that only examine patterns near the decision boundary, which is a more appropriate end-game strategy.

References

[1] C. M. Bachmann and M. H. Bettenhausen, "PURSUIT: An automatic classification tool for remote sensing data," in *Proc. IGARSS*, Toronto, ON, Canada, 2002.

[2] C. M. Bachmann, T. F. Donato, G. M. Lamela, W. J. Rhea, M. H. Bettenhausen, R. A. Fusina, K. DuBois, J. H. Porter, and B. R. Truitt, "Automatic classification of land-cover on Smith Island, VA using HYMAP imagery," *IEEE Trans. Geosci. Remote Sensing*, vol. 40, pp. 2313–2330, Oct. 2002.

[3] C. M. Bachmann, M. H. Bettenhausen, R. A. Fusina, T. F. Donato, A. L. Russ, J. Burke, G. M. Lamela, W. J. Rhea, B. R. Truitt, and J. H. Porter, "A credit assignment approach to fusing classifiers of multi-season hyperspectral imagery," *IEEE Trans. Geosci. Remote Sensing*, to be published.

[4] J. Boardman, "Post-ATREM polishing of AVIRIS apparent reflectance data using EFFORT: A lesson in accuracy versus precision," in *Summaries of the 7th Ann. JPL Airborne Geoscience Workshop*. Pasadena, CA, 1998.

[5] *ENVI 3.4 User's Guide*, , Research Systems, Inc., Boulder, CO, 2000.

[6] G. M. Foody, "The significance of border training patterns in classification by a feedforward neural network using back propagation learning," *Int. J. Remote Sens.*, vol. 20, no. 18, pp. 3549–3562, 1999.

[7] K. Fukumizu, "Statistical active learning in multilayer perceptrons," *IEEE Trans. Neural Networks*, vol. 11, pp. 17–26, Jan. 2000.

[8] B. Gao and C. O. Davis, "Development of a line-by-line atmosphere removal algorithm for airborne and spaceborne imaging spectrometers," *Proc. SPIE*, vol. 3118, pp. 132–141, 1997.

[9] J.-N. Hwang, J. J. Choi, S. Oh, and R. J. M. II, "Query-based learning applied to partially trained multilayer perceptrons," *IEEE Trans. Neural Networks*, vol. 2, pp. 131–136, Jan. 1991.

[10] J. H. Juang and S. Katagiri, "Discriminative learning for minimum error classification," *IEEE Trans. Signal Processing*, vol. 40, pp. 3043–3054, Dec. 1992.

[11] T. Kohonen, *Self Organizing Maps*, 2nd ed. Berlin, Germany: Springer-Verlag, 1997.

[12] J.-M Park and Y. H. Hu, "Adaptive on-line learning of optimal decision boundary using active sampling," in *Proc. 1996 Workshop Neural Networks for Signal Processing VI*, S. Usui, Y. Tohkura, S. Katagiri, and E. Wilson, Eds., Kyoto, Japan, 1996, pp. 253–262.

[13] M. D. Richard and R. P. Lippman, "Neural network classifiers estimate Bayesian a posteriori probabilities," *Neural Comput.*, vol. 3, pp. 461–483, 1991.

[14] D. E. Rumelhart, G. E. Hinton, and R. J. Williams, "Learning internal repreentations by error propagation," in *Parallel Distributed Processing, Explorations in the Microstructure of Cognition*, D. E. Rumelhart and J. L. McClelland, Eds. Cambridge, MA: MIT Press, 1986, vol. 1, Foundations, pp. 318–362.

[15] K. Yamauchi, N. Yamaguchi, and N. Ishii, "An incremental learning method with relearning of recalled interfered patterns," in *Proc. 1996 Workshop Neural Networks for Signal Processing VI*, S. Usui, Y. Tohkura, S. Katagiri, and E. Wilson, Eds., Kyoto, Japan, 1996, pp. 243–252.

Charles M. Bachmann (M'92) received the A.B degree from Princeton University, Princeton, NJ, in 1984, and the Sc.M. and Ph.D. degrees from Brown University, Providence, RI, in 1986 and 1990, respectively, all in physics.

While at Brown University, he participated in interdisciplinary research in the Center for Neural Science, investigating adaptive models related to neurobiology and to statistical pattern recognition systems for applications such as speech recognition. In 1990, he joined the Naval Research Laboratory (NRL), Washington, DC, as a Research Physicist in the Radar Division, serving as a Section Head in the Airborne Radar Branch from 1994 to 1996. In 1997, he moved to the Remote Sensing Division, where he is currently Head of the Coastal Modelling Section of the new Coastal and Ocean Remote Sensing Branch. He has been a Principal Investigator for projects funded by the Office of Naval Research, and more recently for an internal NRL project that focused on coastal land-cover from hyperspectral and multisensor imagery. His research interests include image and signal processing techniques and adaptive statistical pattern recognition methods and the instantiation of these methods in software. His research also focuses on specific application areas such as multispectral and hyperspectral imagery, field spectrometry, SAR, and multisensor data as these apply to environmental remote sensing, especially wetlands and coastal environments.

Dr. Bachmann is a member of the American Geophysical Union, the Society of Wetland Scientists, and the Sigma Xi Scientific Research Society. He is the recipient of two NRL Alan Berman Publication Awards (1994 and 1996), and an Interactive Session Paper Prize at IGARSS '96.